

# A Flexible and Transparent Wearable Antenna Developed with Liquid Dielectric and Polymer

Abu Sadat Md. Sayem 

Department of Electrical and Electronic Engineering, Rajshahi University of Engineering and Technology, Rajshahi 6204, Bangladesh.

Correspondence should be addressed to Abu Sadat Md. Sayem; [sayem061001@gmail.com](mailto:sayem061001@gmail.com)

Received 18 December 2024;

Revised 4 January 2025;

Accepted 19 January 2025

Copyright © 2025 Made Abu Sadat Md. Sayem. This is an open-access article distributed under the Creative Commons Attribution License, which permits unrestricted use, distribution, and reproduction in any medium, provided the original work is properly cited.

**ABSTRACT-** This article proposes the design and realisation of a conformal and transparent antenna compatible for wearable applications. This new antenna utilises water, transparent polymer and conductive fabric for its design and realisation. The topology of the fabricated antenna is deformable and has broadside radiation pattern, thus, suitable for on-body applications which is validated through experimental investigations. The basic antenna comprises a monopole radiator backed by a dielectric reflector which directs the omnidirectional radiation of the monopole to broadside. The notable features of this new antenna are its excellent optical transparency, conformality, good bandwidth, gain and efficiency and the utilisation of easily accessible and bio-friendly materials. The center resonance frequency of the antenna is 2.45 GHz ISM band with 3.42 dB peak gain and 51% efficiency. The usability of the antenna for wearable applications is checked by on-phantom measurements, bending tests and investigating specific absorption rate (SAR). Due to its amazing optical transparency, structural deformability, radiation characteristics, size and ease of fabrication, this antenna is a promising candidate for flexible transparent electronic systems, including wearable body-area networks.

**KEYWORDS-** Broadside, conductive fabric, flexible antennas, monopole, polydimethylsiloxane, robust.

## I. INTRODUCTION

In addition to traditional short and long-haul telecommunication systems, now-a-days antennas are found in health-care, surveillance, national security, emergency departments, satellite systems and so on [1] [2]. With the rising applications, there is a significant change in antenna designs and fabrications. Emerging new applications demand specific antenna characteristics to be compatible in particular application; for example, wearable antennas must be conformal, robust, lightweight and small [3]; antennas mounted on glasses, solar panels and car wind-shields should be transparent. In some applications, such as wearable systems in healthcare, security, military and hands-free applications, it is also recommended to have antennas that are fully or partially unobtrusive and can be mounted conformally on various curved surfaces [4].

Wearable antenna has become one of the most prominent components of the fifth generation (5G) technology which comprises a lot of high added value services [5]. Some critical design factors have made the realisation of wearable antennas some sort of challenging. The challenges are: choosing appropriate materials, antenna properties alteration by the presence of human body [6], antenna performance degradation by bending, stretching and twisting of the antenna geometry for the frequent movement of the wearers and unpleasant environmental stress.

Fabricating unobtrusive wearable antennas is a topic of interest for antenna researchers. Wearable antennas placed under wearers' cloth is the easiest method of hiding antennas' appearance, but the cloth distorts the radiation characteristics of the antenna, thus, this method is not a very desired one [7]. Antennas directly embroidered with wearers' cloth is another approach of hiding antennas' appearance, but this approach is also suffering from the drawback of antennas performance degradation after repeated washing the cloth. Besides these techniques, the efficient alternative is realizing optically transparent and flexible antennas which is easily disguised with surrounding [8]. However, research on transparent and flexible antennas are limited in the literature because of the high level of fabrication challenge and limited scope for material selection. Polydimethylsiloxane (PDMS), Polyethylene terephthalate (PET) and Polyimide are the widely used dielectric materials in transparent antennas. The most popular metals used for transparent antenna fabrication are transparent thin films such as AgHT-4 [9], fluorine-doped tin oxide (FTO) [10], indium-tin-oxide (ITO) [11], Silver Oxide [12], zinc and silver (Ag) mixed ITO (IZTO/Ag/IZTO) film [13]. Mesh conductors such as Tortuous Cu micromesh [14] and mesh fabrics [15][16][17][18] are also reported as effective metals for fabricating see-through antennas. Transparent liquid metal Gallium-Indium eutectic (EGaIn) has been recently utilized successfully to develop wearable antenna [19]. Among these transparent conductors, transparent thin films and mesh conductors each group suffers from the limitation of inverse relationship between electrical conductivity and optical transparency, i.e., with increasing transparency, electrical conductivity is proportionately sacrificed, because of this drawback, transparent antennas suffer from poor RF performance. Table 1 summarizes the

sheet resistance and optical transparency of commonly used transparent conductors. It can be noticed that transparent conductors suffer either from poor electrical conductivity or low optical transparency. It is hard to achieve simultaneously good electrical conductivity and optical transparency. Moreover, it is hard to find transparent conductors which have flexible geometry and they often need structural modification to increase the flexibility and robustness in bending operations. Costly fabrication process often becomes a problem in realizing flexible transparent antennas, especially thin film

conductors suffer from this limitation. For many applications which need highly flexible and robust antenna structure, low cost and easy fabrication, alternative materials and fabrication methods are desired to explore. Water is recently gaining attention in fabricating antennas [24][25][26][27]. Water is almost available everywhere, it is fully transparent, affordable, biocompatible and easy to utilize in antenna realization. In antenna realization, water is utilized either as a dielectric material or as a conductive material. Distilled or pure water has limited electrical conductivity and high relative permittivity, pure

Table 1: Properties of some popular Transparent Conductor

S.no	Material	$R_s$ ( $\Omega/sq$ )	T (%)
1.	Indium-tin-oxide (ITO) [20]	8.6	86
2.	Multi-layered ITO (IZTO/Ag/IZTO) film [13]	4.99	81.1
3.	Fluorine-doped tin oxide (FTO) [21]	4.81	69.2
4.	Silver-coated polyester (AgHT-8) film [22]	8	80
5.	Tortuous copper micromesh [14]	0.07	32
6.	Silver grid layers (AgGL) [23]	0.018	54.5

water is used in antennas where water is used as the dielectric component of the antenna. By dissolving salt, the conductivity of the water can be significantly modified, salt-dissolved water is used in antennas where water acts as the conducting medium. Different types of antennas have been developed utilizing both pure and salt water. A monopole water antenna with a dielectric layer was proposed in [28] where salt water was used for its conducting monopole. [29][30][31] also reported monopole antennas designed with salt water. An efficiency enhanced salt-water monopole antenna was developed in [32]. Most of the earlier versions of pure/distilled water antennas operated on the principle of dielectric resonator (DR) [33][34][35]. Apart from using either pure water or salt water, antennas have also been developed using both types of water for better performance. [36] designed a monopole antenna using both distilled water and salt water in coaxial dual-tube topology which had increased bandwidth and efficiency. Water is most popular for realising reconfigurable antennas. Different types of reconfigurable water antennas are reported in the literature. A pattern reconfigurable water antenna was designed in [37] where a reflector plane was realised with tunable water grating. A polarization-reconfigurable spiral antenna was developed in [38] which used water. A reconfigurable leaky-wave water antenna was developed in [39] which used a periodic water grating. [40] developed a frequency-reconfigurable inverted-L water antenna.

Water antenna operating on a new principle named dense dielectric patch antenna (DDPA) was introduced in [41] which had wideband performance. The antenna occupied 350 mm ( $\sim 1.09 \lambda_0$ )  $\times$  350 mm ( $\sim 1.09 \lambda_0$ )  $\times$  19 mm ( $\sim 0.059 \lambda_0$ ).

The demonstrated antenna was designed for 0.93 GHz frequency, it had impedance bandwidth of 8%, peak gain

of 7.3 dBi and nearly 60% radiation efficiency. The antenna itself was optically transparent, but it required a metallic ground plane which was opaque. Two-year later, [42] developed a new antenna which had water-made patch and water-made ground plane and water was held by see-through plexiglass; by avoiding metal ground, the antenna was able to maintain its optical transparency. This new water patch antenna operated at 2.4 GHz frequency with 35% 10-dB impedance bandwidth, 4 dBi peak gain and 82% efficiency and it had omnidirectional conical beam radiation patterns. The antenna occupied a diameter of 306 mm ( $\sim 2.45 \lambda_0$ ) and a height of 7.6 mm ( $\sim 0.3 \lambda_0$ ). The first flexible, transparent and durable water-based antenna was developed in [8]. The demonstrated antenna had a dipole feed backed by water reflector which made the antenna unidirectional and compatible for wearable applications. The dipole was made with conductive fabric and water holder was made with flexible polymer Polymethyl-siloxane (PDMS) which has a unique characteristic of amazing flexibility, light transparency, thermal and chemical stability [43] [44]. The antenna had excellent transparency, flexibility and good RF performance, but had comparatively narrow bandwidth. Following this work, in this paper, a flexible, transparent and durable water-based antenna is developed with improved bandwidth and an improvement in feeding topology. The realized antenna is structurally deformable and highly transparent compared to the conventional water antennas, this antenna is miniature in size, which is achieved through its unique operating principle. Other water antennas operate as monopole radiator using salt water, dielectric resonator antenna using pure water or dense dielectric patch antenna using pure water. Instead of using any of this technique, the proposed design has used a monopole antenna as the main radiator which is

backed by a pure water reflector to form unidirectional radiation. By using this mechanism, broadside water antenna is realized to have a small size. Moreover, the fabrication of the proposed antenna is free from the requirement of expensive materials and complicated procedure.

The demonstrated antenna occupies a net dimension of 60 mm length, 60 mm width and 14.5 mm height ( $\sim 0.49 \lambda_0 \times 0.49 \lambda_0 \times 0.11 \lambda_0$ ). The compatibility of the new antenna

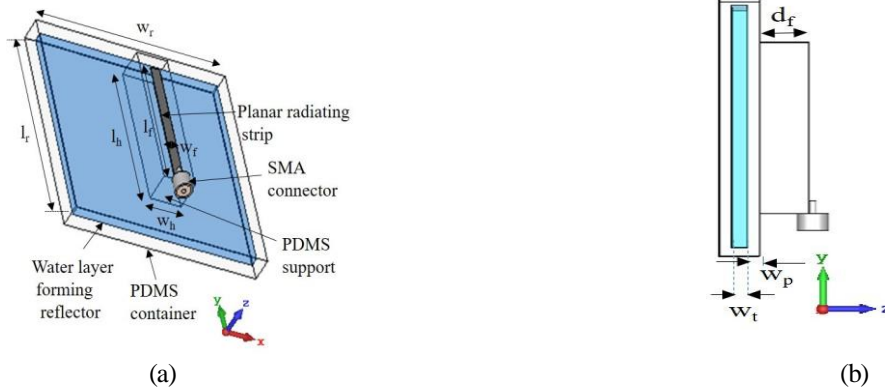


Figure 1: Antenna structure-(a) perspective view, (b) side view.

Table 2: Dimensions of the Antenna Topology

Parameter	Description	Value (mm)
$l_r$	Water layer's length	56
$w_r$	Water layer's width	56
$w_t$	Water layer's thickness	2.5
$w_p$	Thickness of the hollow box	2
$l_h$	PDMS support's length	40
$w_h$	PDMS support's width	10
$d_f$	PDMS support's height	8
$l_f$	Length of the monopole	34.5
$w_f$	Width of the Monopole	3

## II. ANTENNA STRUCTURE AND OPERATING MECHANISM

### A. Structure of the Antenna

The details structure of the proposed antenna is shown in Figure 1. As can be seen from this geometry, the principal radiator is a planar narrow monopole which is built with highly conductive fabric NCS95R-CR, from Marktek Inc., this conductive fabric is 0.13 mm thick and it has a sheet resistance of  $0.01 \Omega/\text{sq}$ . The radiating monopole is connected to an SMA connector at one side for feeding purpose. A rectangular reflector plane, made with pure water, is placed below the monopole radiator at a certain distance apart, the water is placed inside a PDMS-made rectangular box. Here, the function of the reflector plane is to convert the omnidirectional radiation of the monopole to broadside unidirectional pattern. Antennas having unidirectional pattern is important for on-body applications because of its low interaction with human body (this antenna radiates away from the body and the radiation towards body is very low). Another rectangular block made

for applications near lossy human body is also studied in this paper.

The rest of this paper is organized as follows: Section II describes the antenna configuration and operation, in Section III parametric studies are conducted; Section IV briefly describes the fabrication process; Section V contains the predicted and measured results and finally the Conclusion is depicted in Section VI. CST Microwave studio 2021 was used for all the simulations in this paper.

with PDMS is mounted on the hollow box which acts as a supporting structure for the monopole radiator. Pure water used in the design had a measured dielectric constant of 78 at the target frequency of 2.45 GHz. The dielectric property of the PDMS was tested by Agilent 85070E Dielectric Kit, the measured dielectric constant was 2.75 which was almost constant for 0.5 to 10 GHz frequency, whereas the loss tangent increased gradually from 0.008 to 0.07 in this frequency band. The dimensions of the antenna topology are shown in Table 2.

This antenna has a very high flexible structure because it is built with all flexible materials, i.e., water holder is made with PDMS, water itself is liquid, monopole is built with flexible conductive fabric, support block to hold the monopole is built with PDMS. Moreover, the antenna has high optical transparency. Thus, this antenna is highly flexible and transparent, and excellent candidate for unobtrusive wearable applications. In contrast to the developed flexible water antenna in [8], the proposed antenna has significant structural improvement for wearable applications. In the antenna developed in

[8], the SMA connector was located at the middle of the antenna topology which required the feeding co-axial cable to go to the middle of the antenna topology passing on top of the water reflector which not only incorporated complexity in wearable applications but also hampered unobtrusiveness. In this new antenna, the SMA connector is located nearly at the edge of the antenna, thus, the feeding co-axial cable only needs to come at the edge which simplified the feeding process in wearable applications and does not jeopardize the unobtrusiveness.

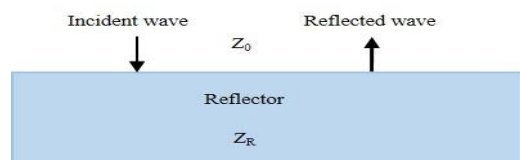


Figure 2: Reflection of a plane wave from a high permittivity reflector surface.

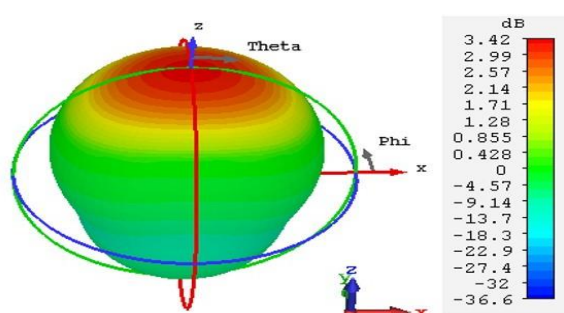


Figure 3: 3-D radiation pattern of the proposed antenna plotted for 2.45 GHz demonstrating broadside radiation.

### B. Operating Mechanism

According to Fresnel's equations as mentioned in [45], a plane wave is reflected from the intersection of the two mediums having high contrast of relative permittivity as illustrated in Figure 2. The proposed antenna operates according to this principle. Here, water layer is located underneath a planar monopole radiator, as the permittivity of the water is very high (nearly 78) compared to PDMS (2.75) and surrounding air (1), the radiation from the monopole reflects back from the water surface. This is further explained in [46] and [41], they described that the interfacing surface of two mediums having high dielectric permittivity difference resembles a boundary condition which is very similar to an electric wall; in the proposed design, the plane wave from the monopole is reflected back from the air-water interface (which has a permittivity difference of 78), thus, the radiation becomes unidirectional broadside. The predicted 3-D radiation pattern of the antenna is shown in Figure 3 which is identical to the broadside pattern produced from microstrip patch antenna.

CST Microwave studio 2021 was used for the simulation analysis of the antenna design. The dimension of the water layer is responsible for the reflection of the electromagnetic wave coming from the monopole, which in effect determines how the antenna behaves more likely as a patch antenna. The impact of the water layer's dimension on antenna's radiation behaviour is analysed later in parametric study section. However, optimum value is selected to make the antenna structure smaller in size

which is also a major concern in this antenna design. The distance between the top surface of the water layer and the monopole controls the gain of the antenna which is described in next section.

The magnitude of current distribution and the magnitude of electric field (E-field) distribution are shown in Figure 4 and Figure 5, respectively. As shown in Figure 4, current only flows through the radiator and Figure 5 illustrates the effect of water layer and the PDMS container on the E-field distribution.

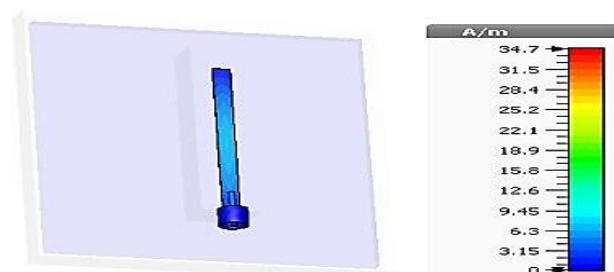


Figure 4: Absolute value of the current distribution in the antenna.

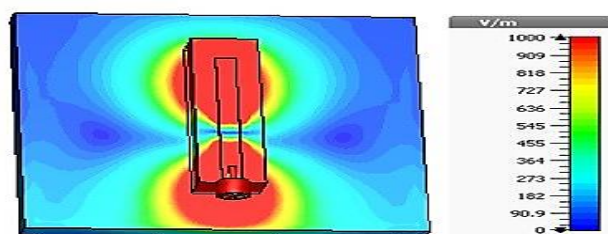


Figure 5: Absolute value of the electric field distribution in the antenna.

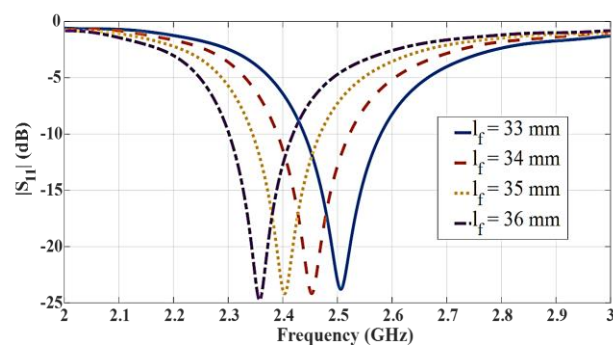


Figure 6: Effect of the length of radiator on resonance frequency.

### III. ANTENNA PARAMETERS ANALYSIS

The RF performance of the antenna is dependent upon the dimension of the water reflector. The major parameters that control antenna's radiation behaviour are the length, width and thickness of the water layer and the distance from the water layer to the monopole. Details simulation investigations have been accomplished to check the impact of these parameters and the results are briefly presented in the following subsections. All the presented results are for 2.45 GHz frequency. For observing the effect of a particular parameter, the remaining parameter values are considered as in Table 2.

**A. Study the impact of monopole radiator's length**

Monopole radiator's length mainly controls the antenna's center resonance frequency. The impact of the variation of the length of the monopole is illustrated in Figure 6 which shows that the resonance position shifts towards lower frequency band with the increase of the length.

**B. Study the impact of the length of the water layer on antenna performance**

The effects of the length of the water layer on radiation patterns are illustrated in Figure 7 which shows how the larger length of the water shifts the radiation from omnidirectional to unidirectional pattern; with the increase of the length, the back radiation reduces and the front radiation increases and the radiation behaves more likely as a patch antenna rather than the original omnidirectional monopole.

The front to back ratio (F/B) of the radiation patterns of the antenna for different length of the water reflector are shown in Table 3. It shows that at 36 mm length of the water reflector, the front to back ratio (F/B) is negative which is because the maximum radiation goes towards lower hemisphere at this small length of the water reflector where the effect of the PDMS is more than the water, but with the increase of reflector length front to back ratio (F/B) improves which indicates that radiation moves towards upper hemisphere. In our design, upper hemisphere refers to the positive z direction.

Figure 8 demonstrates how antenna gain improves with the increase of the water layer's length.

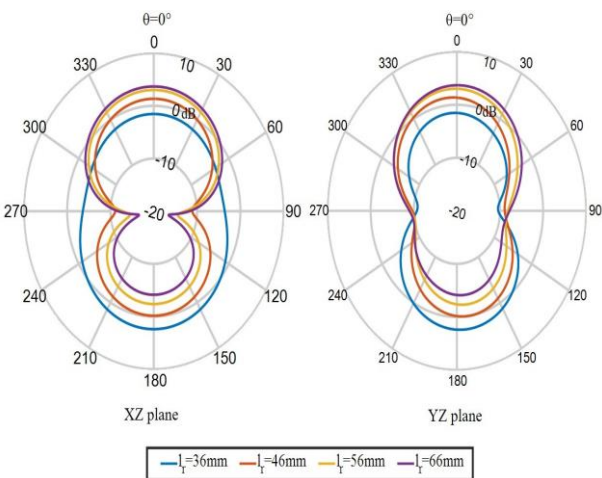


Figure 7: The radiation patterns of the antenna for various length of the water layer.

Table 3: Front to back ratio of the Radiation Pattern of the Antenna for Different Water Layering Length

$l_r$ (mm)	36	46	56	66
F/B (dB)	-2.2	3.7	6.1	7.7

**C. Study the impact of the width of the water layer on antenna performance**

The width of the water layer affects the radiation patterns and gain of the antenna like the length of the water layer.

Table 4: Front to back ratio of the Antenna for Different Water Layer Width

$w_r$ (mm)	36	46	56	66
F/B (dB)	-3	5.1	5.4	5.6

Figure 9 depicts that wider water layer shifts the radiation closer to broadside direction from monopole like radiation. The front to back ratio (F/B) of the radiation patterns of the antenna for varying water reflector width is shown in Table 4. It shows that at 36 mm width of the water reflector the front to back ratio (F/B) is negative which is because the maximum radiation goes to lower hemisphere for this small width of the water layer. When the width is increased then front to back ratio becomes positive which confirms the shift of the radiation towards broadside. Further widening the reflector width improves the front to back ratio (F/B) accordingly.

Figure 10 demonstrates how antenna gain improves with the increase of the water layer's width.

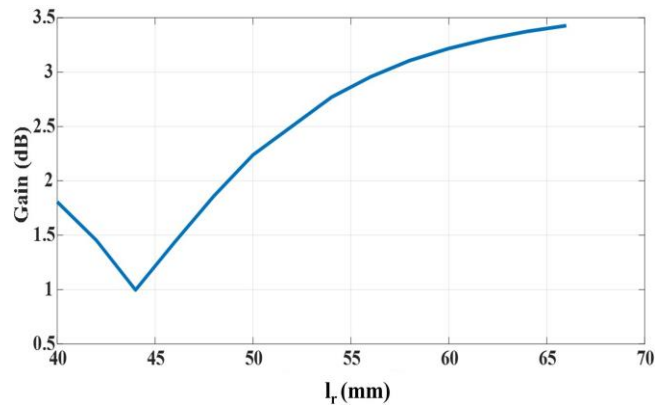


Figure 8: The gain of the antenna for various length of the water layer.

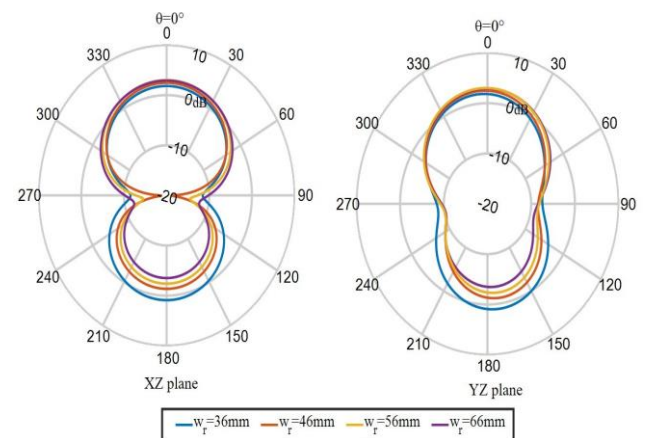


Figure 9: The radiation patterns of the antenna for various width of the water layer.

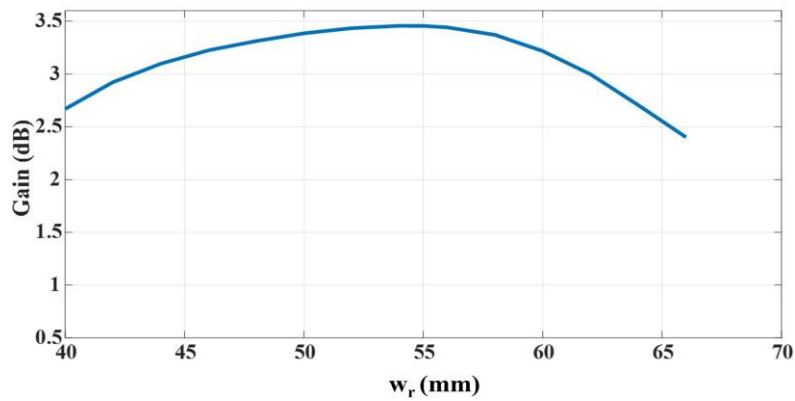


Figure 10: The gain of the antenna for different width of the water layer.

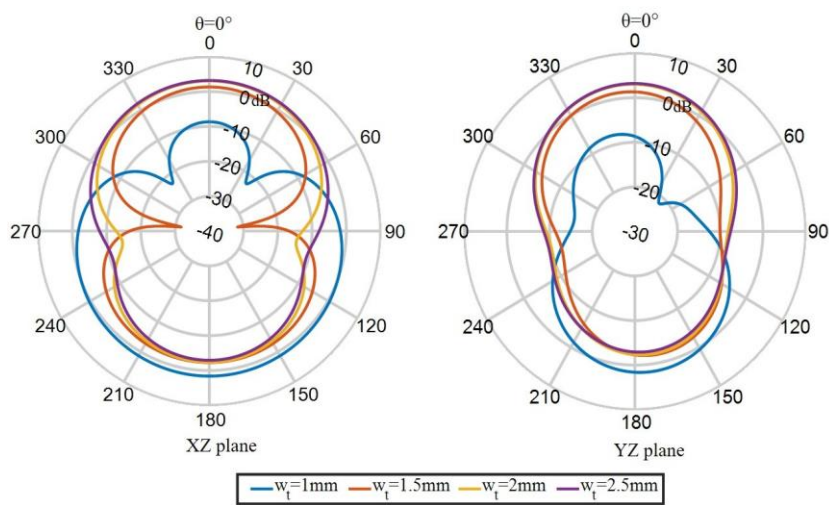


Figure 11: The radiation patterns of the antenna for very thin to thicker water layer.

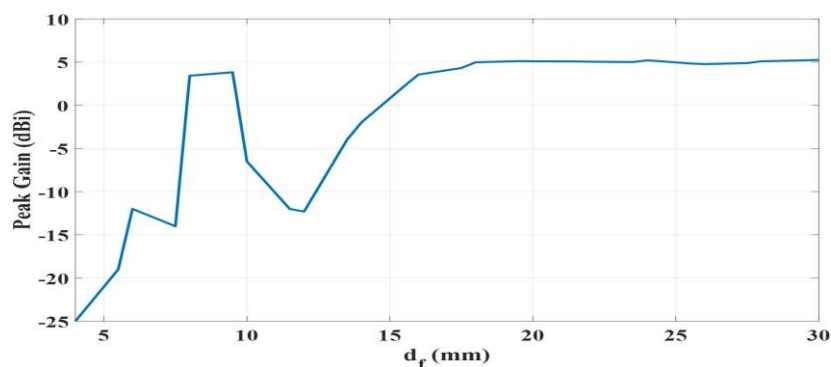


Figure 12: The gain of the antenna for gradually increasing the thickness of the water layer

**D. Study the impact of the thickness of the water layer on antenna performance**

Figure 11 and Figure 12 depicts the impacts of the thickness (height) of the water layer on the radiation patterns and gain of the antenna, respectively. Thicker water layer contributes to stronger reflection and improves broadside radiation. In contrast, very thin water layer leaks the radiation towards backside ( $\theta = -90^\circ$ ). The front to back ratio (F/B) of the radiation patterns

of the antenna for four different water layer thickness is shown in Table 5. It shows that for a small 1 mm thick water layer, the front to back ratio (F/B) is negative, thickening the water layer moves the radiation towards upper hemisphere.

**E. Study the effects of the distance between the radiator and reflector**

The position of the monopole on top of the reflector has

significant impact on the gain and radiation efficiency of the antenna. Figure 13 depicts how antenna gain is impacted by varying the distance from the reflector to radiator. It can be noted that when the distance between the radiator and reflector is one-quarter of the wavelength, there will be a superimposed enhancement of radiation in the far field, otherwise there will be cancellation, however, the peak gain does not improve significantly for increasing the distance from 8mm to 30mm. In final antenna design, optimized distance (8 mm. i.e.,  $\sim 0.07 \lambda_0$ ) is maintained which is not one-quarter of

the wavelength, this distance is selected to keep the antenna height small, increasing it to one quarter of the wavelength would drastically increase the height of the antenna and make it impractical for wearable applications.

Table 5: Front to back ratio of the pattern of the Antenna for Different Water Layer Thickness

wt (mm)	1	1.5	2	2.5
F/B (dB)	-10.3	3.6	5.4	6.1

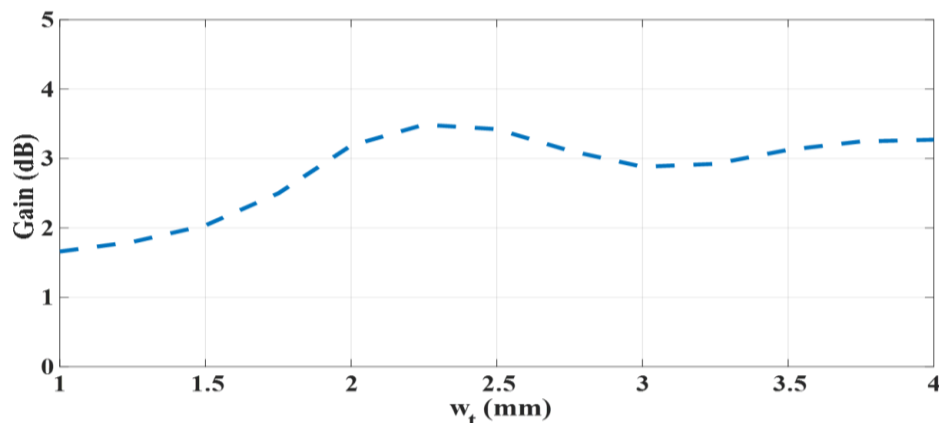


Figure 13: Antenna gain for varying the distance between the radiator and the reflector

#### IV. ANTENNA FABRICATION

The antenna was fabricated by using customized molds which was made by using 3-D printing technology. The demonstrated fabrication method was less costly, easily customizable and scalable. Figure 14 (a) illustrates the structure of the molds. Three 3-D printed molds were used to fabricate the hollow rectangular box with PDMS and the supporting rectangular PDMS block. The model of the utilized 3-D printer was Form 2 which was manufactured by Formlabs, this 3-D printer uses Stereolithography (SLA) printing mechanism, photopolymer resin was used as the printing material. The printing setting was as follows: density 1.00, point size 0.60 mm, base thickness 3.00 mm, height above base 5.00 mm, resolution 0.5 mm. The required printing time was 5 hour 42 minutes and total number of layers were 220. After finishing the printing, the printed structures (molds) were flushed by Isopropanol (IPA) (Sigma-Aldrich) jet to remove the residual resin, then Digital Ultrasonic Cleaner (JP 4820, Skymen) was used for sonication, finally, the stickiness was cured by a heating and drying oven (UF-55, Memmert) set at 75°C overnight.

After fabricating the molds, PDMS solution was prepared by mixing base and curing agent by maintaining 10:1 ratio, Dow Corning's Sylgard 184 silicone elastomer kit was used for preparing PDMS solution. After preparing the PDMS solution, it was poured on the molds, desiccated in a vacuum desiccator and then cured at 65°C for 2 hours in an oven. Fully cured PDMS was a flexible structure which was carefully peeled off from the molds. The hollow PDMS water holder was made with the cured PDMS blocks from mold 1 and mold 2 and the PDMS supporting block was made from the cured PDMS blocks from mold 3. Figure 14 (b) shows the photographs of the cured PDMS structures after peeling off from the molds. In Figure 14

(b), PDMS layer 1, PDMS layer 2 and PDMS layer 3 were peeled off from mold 1, mold 2 and mold 3, respectively. The cured PDMS layer 1 obtained from mold 1 was like a box without a cover. PDMS layer peeled-off from mold 2 was attached on top of this structure to make the hollow PDMS holder. The cured PDMS peeled-off from mold 3 was then glued by small amount of PDMS solution to the upper surface of this hollow box.

After making the box and PDMS support block, the conductive fabric NCS95R-CR was cut by a sharp razor according to the dimension in Figure 1 to make the monopole which was then placed on top of the supporting PDMS block by small amount of uncured PDMS and cured in an oven at 65°C for 2 hours. After completing the fabrication of the monopole and water holder, an SMA connector was connected at one side of the monopole with silver conductive epoxy which was cured in an oven for two hours at 65°C. Finally, pure water was injected inside the hollow box through the PDMS wall by using a syringe. The photograph of the final prototype of the antenna is shown in Figure 14 (c) which also confirms its optical transparency through the clear visualisation of logo and text. Figure 14 (d) shows that the fabricated prototype has very high flexible structure which can be deformed by avoiding structural distortion. The hollow PDMS container consists of 2mm thick wall, 2mm thick PDMS is selected to avoid possible leakage of water. Due to PDMS's excellent flexibility, this thickness does not interrupt the flexibility of the antenna as depicted in the photo of bending testing shown in Figure 14 (d).

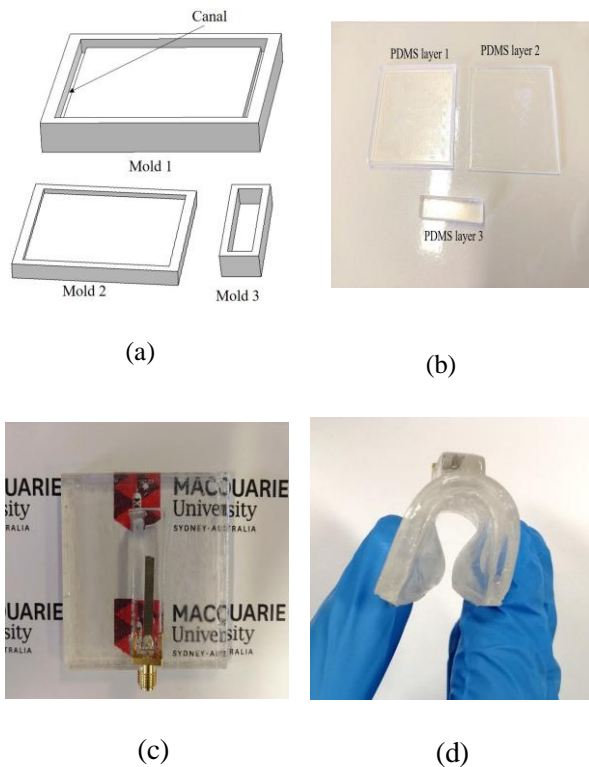


Figure 14: (a) Geometry of the molds, (b) Cured PDMS layers after peeling off from the molds, (c) photograph of

the antenna prototype, (d) Deformed antenna.

## V. ANTENNA PERFORMANCE TESTING

A thorough performance investigation of the simulated results and the measured results of the prototype demonstrate the feasibility of the antenna in real-life applications. In this paper, the predicted results refer to simulated results.

Figure 15 illustrates the magnitude of input reflection coefficient ( $|S_{11}|$ ) both for the predicted results extracted from simulation and the results got from measurement, a comparison of these results depicts that the measured performance follows the predicted results very well. The parameter  $|S_{11}|$  was measured by a Power Network Analyser (PNA) of model N5242A PNA-X manufactured by Agilent Technologies. The measured  $|S_{11}| < -10$  dB bandwidth of the antenna was 470 MHz. The antenna in [8] had a bandwidth of 170 MHz, so a significant improvement of bandwidth is visible in this new design.

The developed water antenna is not only optically transparent and flexible but also wearable on human body. The compatibility of the antenna for on-body operation was checked by testing its performance on a custom made ultra-wideband (UWB) semi-solid phantom which has similar properties of human muscle tissue. The phantom had a dimension of  $200\text{mm} \times 200\text{mm} \times 47\text{mm}$  which was fabricated according to the procedure described in [47]. The components of the phantom are: deionized

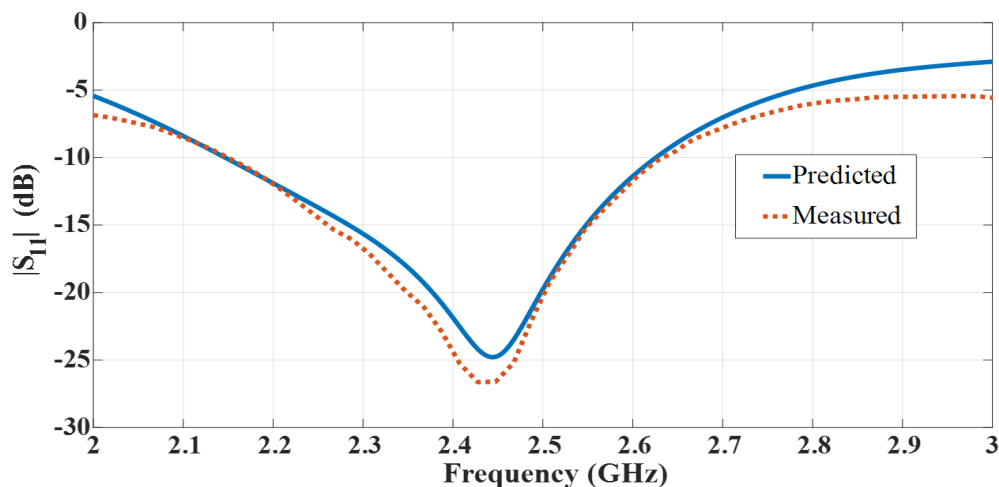


Figure 15: Predicted and measured  $|S_{11}|$  parameter of the developed antenna

water (85.15%), agar (2.64%), polyethylene powder (PEP) (10.52%), sodium chloride (0.18%), TX-151 (1.46%) and sodium dehydro-acetate (0.05%). Figure 16 (a) shows the test set-up with phantom.

The antenna was bent and placed on the wrist of a human hand shaped phantom comprising a bending radius of nearly 28 mm as shown in Figure 16 (b) and (c) to measure the bending performance on human-body environment. This structure of the phantom was achieved by filling hollow hand of a mannequin with the same materials used for the rectangular phantom shown in Figure 16(a). Figure 17 depict the measured  $|S_{11}|$  results for on-air testing, on flat phantom testing and bending testing. It is observed that the phantom has

impact on the resonance position as well as impedance matching. However, the resonance frequency shifts only a small amount and the impedance matching is good which subsequently assures that the antenna is compatible for placement on different curved surfaces on human body. The measured  $|S_{11}| < -10$  dB bandwidth on flat phantom is 360 MHz. Figure 17 also illustrates that the resonance frequency moves towards lower band under bending particularly when bent along the length of the antenna, this effect comes from the increased current path upon prolonging length of the monopole radiator in bending that the antenna structure is highly flexible and operations.

The far-field radiation patterns of the antenna are plotted in Figure 18. NSI700S-50 spherical near-field

antenna range was used for measuring the far-field patterns of the antenna. The predicted and measured normalized patterns plotted in Figure 18 indicates that the antenna radiates broadside similar to a microstrip patch antenna backed by full-ground plane, the results validate the proposed method of designing unidirectional antenna with monopole and water reflector. The measured peak gains of the antenna from 2.2 to 2.5 GHz are plotted and compared with the predicted gains in Figure 19. At 2.45 GHz, a measured peak gain of 2.94 dB is achieved with an efficiency of 51%. A little error is visible between the measured and predicted results, this happens due to the impact of fabrication inaccuracy. Moreover, some air bubbles remained in water despite using vacuum desiccator, which also affected the result. The SMA connector was connected to the conductive fabric with silver epoxy, extra epoxy remains around the SMA connector also affects the results in anechoic chamber measurement.

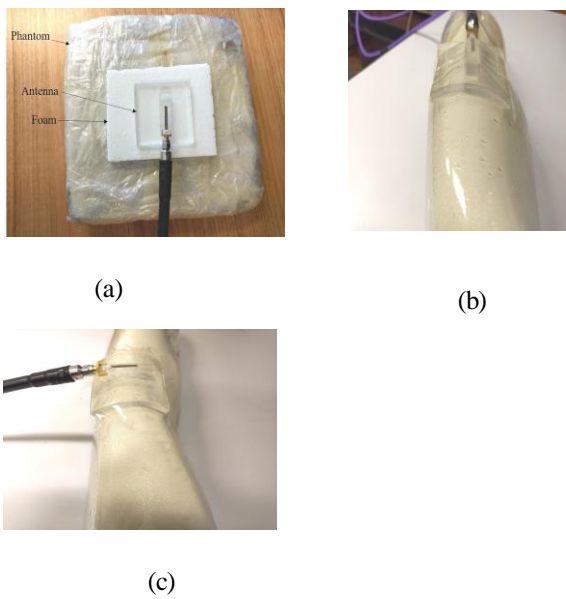


Figure 16: Photographs of the antenna on phantom and bending test-(a) on rectangular phantom, (b) bent on human hand shaped phantom along the width, (c) bent on

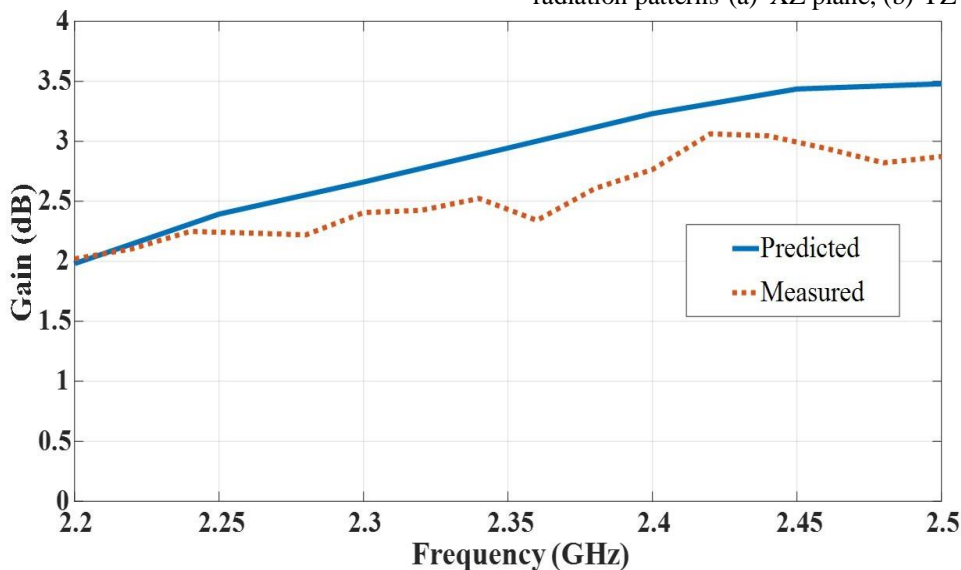
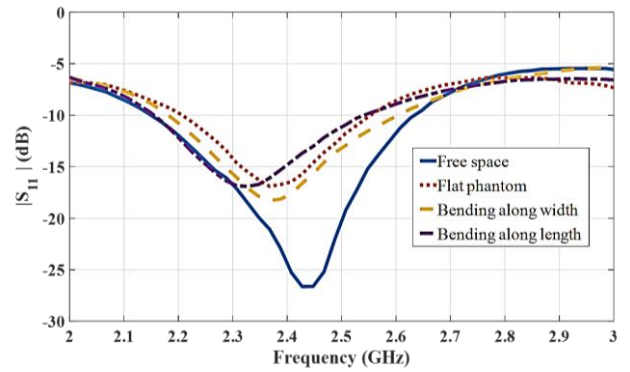


Figure 19: Predicted and measured peak gain of the proposed antenna over the operating band



human hand shaped phantom along the length.

Figure 17: Measured  $|S_{11}|$  of the antenna on flat phantom and under bending.

The Specific Absorption Rate (SAR) of the antenna was numerically calculated to investigate the effect of its radiation on human body and thus its compliance for wearable applications. The SAR level of the antenna was calculated in CST Microwave Studio 2021. In the simulation setting, 5 mm gap was maintained between the antenna and the muscle tissue having a dimension of 200 mm × 200 mm × 47 mm, 0.1 W input power was applied for the calculation and the SAR was averaged over 10 g of tissue. The numerically calculated

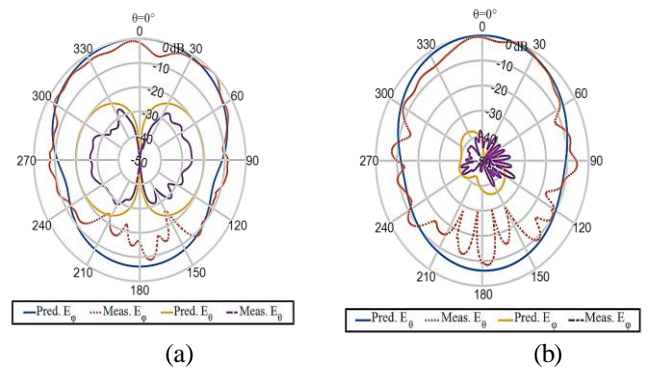


Figure 18: Predicted and measured normalized far-field radiation patterns-(a) XZ plane, (b) YZ plane

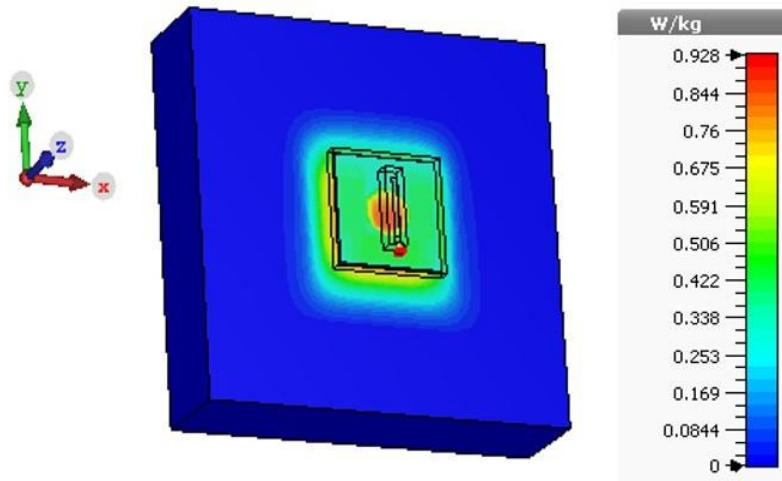


Figure 20: The distribution of SAR at 2.45 GHz frequency in homogeneous muscle tissue, computed using CST Microwave Studio 2021

maximum SAR was 0.93 W/kg which is obviously smaller than the recommended 2 W/kg SAR limit according to IEEE C95.1-2005 standard. So, the water reflector limits the back radiation which acts similar to the ground plane of the patch antenna. It is clear that this flexible water antenna can be safely used in wearable applications. Figure 20 shows the predicted SAR distribution in the human muscle equivalent phantom which explicitly indicates the function of the water reflector to protect the phantom from electromagnetic exposure. So, the proposed water antenna

can be used like a flexible and wearable patch antenna with full ground plane. Finally, a comparison is made among the demonstrated antenna and the state-of-the-art transparent wearable antennas reported in the literature to demonstrate the significance of the proposed design. Table 6 depicts this comparison. In the comparison, the resonance frequency, dimension of the antenna, type of the antenna, gain, efficiency, conductor and dielectric used in the antenna geometry are taken into consideration.

Table 6: Comparison of the Demonstrated Antenna with Transparent Wearable Antennas Reported in the Literature

Ref.	Freq. (GHz)	Dim. ( $\lambda_0^3$ )	Antenna Type	Gain (dBi)	Effi (%)	Conductor	Dielectric	Trans. (%)
[8]	2.45	$0.49 \times 0.49 \times 0.11$	Dipole	3.2	51	Conductive Fabric	PDMS/Water	94%
[12]	3.19-9.30	$0.47 \times 0.58 \times 0.01$	MIMOss Patch	2.49	40	Silver Oxide	PET	70
[13]	2.45	$0.21 \times 0.016 \times -$	Monopole	2.89	34.8	IZTO/Ag/IZTO film	Polyimide	81.1%
[14]	2.92	$0.08 \times 0.11 \times 0.004$	CPW Patch	-0.02	81.4	Tortuous Cu micromesh	PDMS	32%
[16]	4.7	$0.94 \times 0.94 \times 0.0031$	Slot	3.8	85	Metallic mesh	PET	93%
[17]	0.868	$0.22 \times 0.13 \times 0.003$	Loop	-15.3	1.66	Conductive Fabric	PDMS	72%
[18]	2.4	$0.48 \times 0.48 \times 0.02$	Patch	2.5	42.26	Conductive Fabric	PDMS	72%
[19]	2.45, 5.8	$0.38 \times 0.38 \times 0.02$	Slot	-1.76, 3	15, 25	EGaIn	PDMS	43%
[48]	2.38-2.67	$0.49 \times 0.49 \times 0.11$	Folded Dipole	2.45-4.25	48.3-57.7	Conductive Fabric	PDMS/Water	94%
This work	2.45	$0.49 \times 0.49 \times 0.11$	Monopole	3.42	51	Conductive Fabric	PDMS/Water	94%

It can be noticed from the comparison that most of the transparent wearable antennas suffer from poor gain and radiation efficiency, this happens due to the high resistance of the transparent conductors. There is a trade-off between the optical transparency and sheet resistance of the transparent conductors, so efficiency and gain should be sacrificed if it is intended to maximise the optical transparency. In contrast to transparent conductors, water is an effective alternative material due to its high level of optical transparency, availability, biocompatibility and excellent dielectric properties. However, water antennas are bulky in size, so not suitable for wearable applications. The reported water antennas in the literature work on the principle of dielectric resonator (DR) or dense dielectric patch antenna using pure water or use salt water for working as monopole radiator. [8] and [48] proposed new types of water antenna. In the new design, water was enclosed inside polymer made cavity working as reflector surface, the main radiator was planar dipole. [8] was the first reported water antenna that was flexible and small in size and suitable for on body operation. The proposed design of this article follows the same materials and design procedure of this work, but a change is made in the radiating element. Two major advantages are accomplished in the proposed design over [8] as well as [48] the first advantage is that the proposed design provides 470 MHz impedance bandwidth while [8] and [48] had 170 MHz bandwidth, so a clear 2.7 times bandwidth improvement is achieved in the new design, the second advantage is that the proposed antenna has significant structural improvement for wearable applications in term of feeding process. In this new antenna, the SMA connector is located nearly at the edge of the antenna, thus, the feeding co-axial cable only needs to come at the edge which simplifies the feeding process in wearable applications and does not jeopardize the unobtrusiveness.

## VI. CONCLUSION

An optically transparent and flexible antenna having broadside radiation pattern and good impedance bandwidth has been successfully developed in this paper. The antenna operates at 2.45 GHz ISM band with a measured bandwidth of 19.2%, efficiency of 51% and a gain of 3.42 dB. In contrast to other reported transparent antennas, the proposed design is comparatively easy to realize, shows promising RF performance, compatible for direct placement on human body and has mechanical stability in conformal operations. The antenna is realized from water, PDMS and conductive fabric; all of these are flexible materials, low in cost, easily available and easy to process. The proposed cost-effective fabrication process can be a great interest to antenna researchers to realize robust flexible transparent antennas and RF devices. The promising features of optical transparency, flexibility, robustness, geometrical shape and remarkable electrical performance demonstrate that the new antenna is useful in a broad range of applications where optical transparency and flexibility are prime requirements of the systems.

## REFERENCES

- [1] T. Peter, T. A. Rahman, S. W. Cheung, R. Nilavalan, H. F. Abutarboush, and A. Vilches, "A Novel Transparent UWB Antenna for Photovoltaic Solar Panel Integration and RF Energy Harvesting," *IEEE Transactions on Antennas and Propagation*, vol. 62, no. 4, pp. 1844–1853, Apr. 2014. Available from: <https://doi.org/10.1109/TAP.2014.2298044>
- [2] W. Hong, S. Lim, S. Ko, and Y. G. Kim, "Optically Invisible Antenna Integrated Within an OLED Touch Display Panel for IoT Applications," *IEEE Transactions on Antennas and Propagation*, vol. 65, no. 7, pp. 3750–3755, Jul. 2017. Available from: <https://doi.org/10.1109/TAP.2017.2705127>
- [3] P. Nepa and H. Rogier, "Wearable antennas for off-body radio links at VHF and UHF bands: Challenges, the state of the art, and future trends below 1 GHz," *IEEE Antennas and Propagation Magazine*, vol. 57, no. 5, pp. 30–52, Oct. 2015. Available from: <https://doi.org/10.1109/MAP.2015.2472374>
- [4] R. B. Green et al., "Optically Transparent Antennas and Filters: A Smart City Concept to Alleviate Infrastructure and Network Capacity Challenges," *IEEE Antennas and Propagation Magazine*, vol. 61, no. 3, pp. 37–47, Jun. 2019. Available from: <https://doi.org/10.1109/MAP.2019.2907895>
- [5] U. Ali, S. Ullah, B. Kamal, L. Matekovits, and A. Altaf, "Design, analysis and applications of wearable antennas: A review," *IEEE Access*, vol. 11, pp. 14458–14486, 2023. Available from: <https://doi.org/10.1109/ACCESS.2023.3243292>
- [6] N. H. Abd Rahman, Y. Yamada, and M. S. Amin Nordin, "Analysis on the effects of the human body on the performance of electro-textile antennas for wearable monitoring and tracking application," *Materials*, vol. 12, no. 10, p. 1636, 2019. Available from: <https://shorturl.at/QXcfd>
- [7] R. B. V. B. Simorangkir, Y. Yang, K. P. Esselle, and B. A. Zeb, "A method to realize robust flexible electronically tunable antennas using polymer-embedded conductive fabric," *IEEE Transactions on Antennas and Propagation*, vol. 66, no. 1, pp. 50–58, Jan. 2018. Available from: <https://doi.org/10.1109/TAP.2017.2772036>
- [8] A. S. M. Sayem, R. B. V. B. Simorangkir, K. P. Esselle, R. M. Hashmi, and H. Liu, "A Method to Develop Flexible Robust Optically Transparent Unidirectional Antennas Utilizing Pure Water, PDMS, and Transparent Conductive Mesh," *IEEE Transactions on Antennas and Propagation*, vol. 68, no. 10, pp. 6943–6952, 2020.
- [9] H. J. Song et al., "A method for improving the efficiency of transparent film antennas," *IEEE Antennas and Wireless Propagation Letters*, vol. 7, pp. 753–756, 2008.
- [10] N. Guan, H. Furuya, K. Himeno, K. Goto, and K. Ito, "A monopole antenna made of a transparent conductive film," in *2007 International Workshop on Antenna Technology: Small and Smart Antennas, Metamaterials and Applications*, Mar. 2007, pp. 263–266.
- [11] G. Sun, B. Muneer, and Q. Zhu, "A study of microstrip antenna made of transparent ITO films," in *2014 IEEE Antennas and Propagation Society International Symposium (APSURSI)*, Jul. 2014, pp. 1867–1868.
- [12] A. Desai et al., "UWB Connected Ground Transparent 4-Port Flexible MIMO Antenna for IoT Applications," *IEEE Internet of Things Journal*, vol. 11, no. 7, pp. 12475–12484, 2024.
- [13] S. Hong, S. H. Kang, Y. Kim, and C. W. Jung, "Transparent and flexible antenna for wearable glasses applications," *IEEE Transactions on Antennas and Propagation*, vol. 64, no. 7, pp. 2797–2804, Jul. 2016.
- [14] T. Jang, C. Zhang, H. Youn, J. Zhou, and L. J. Guo, "Semitransparent and flexible mechanically reconfigurable electrically small antennas based on tortuous metallic micromesh," *IEEE Transactions on Antennas and Propagation*, vol. 65, no. 1, pp. 150–158, Jan. 2017.

- [15] Q. H. Dang, S. J. Chen, N. Nguyen-Trong, and C. Fumeaux, "Multifunctional reconfigurable wearable textile antennas using coplanar reconfiguration modules," *IEEE Transactions on Antennas and Propagation*, vol. 71, no. 5, pp. 3806–3815, 2023.
- [16] H. Qiu et al., "Compact, flexible, and transparent antennas based on embedded metallic mesh for wearable devices in 5G wireless network," *IEEE Transactions on Antennas and Propagation*, vol. 69, no. 4, pp. 1864–1873, 2021.
- [17] R. B. Simorangkir et al., "Transparent epidermal antenna for unobtrusive human-centric internet of things applications," *IEEE Internet of Things Journal*, vol. 11, no. 1, pp. 1164–1174, 2023.
- [18] A. S. M. Sayem et al., "Flexible and transparent circularly polarized patch antenna for reliable unobtrusive wearable wireless communications," *Sensors*, vol. 22, no. 3, p. 1276, 2022.
- [19] W. Zhu, X. Liu, Y. Fan, Z. Zhang, and X. Ma, "Transparent and flexible antenna with polarization reconfigurability using EGaIn for wearable applications," *IEEE Transactions on Antennas and Propagation*, 2024.
- [20] F. Colombel, X. Castel, M. Himdi, G. Legeay, S. Vigneron, and E. M. Cruz, "Ultrathin metal layer, ITO film and ITO/Cu/ITO multilayer towards transparent antenna," *IET Science, Measurement & Technology*, vol. 3, no. 3, pp. 229–234, May 2009.
- [21] S. Sheikh, M. Shokoo-Saremi, and M. Bagheri-Mohagheghi, "Transparent microstrip patch antenna based on fluorine-doped tin oxide deposited by spray pyrolysis technique," *IET Microwaves, Antennas & Propagation*, vol. 9, no. 11, pp. 1221–1229, 2015.
- [22] S. Y. Lee, M. Choo, S. Jung, and W. Hong, "Optically transparent nano-patterned antennas: A review and future directions," *Applied Sciences*, vol. 8, no. 6, 2018. Available from: <https://www.mdpi.com/2076-3417/8/6/901>
- [23] J. Hautcoeur, F. Colombel, X. Castel, M. Himdi, and E. M. Cruz, "Radiofrequency performances of transparent ultra-wideband antennas," *Progress in Electromagnetics Research C*, vol. 22, pp. 259–271, 2011.
- [24] J. Li et al., "A fan-shaped compact water antenna with wide bandwidth and optical transparency," *IEEE Transactions on Antennas and Propagation*, vol. 70, no. 4, pp. 3017–3021, 2022.
- [25] S. G. O'Keefe and S. P. Kingsley, "Tunability of liquid dielectric resonator antennas," *IEEE Antennas and Wireless Propagation Letters*, vol. 6, pp. 533–536, 2007.
- [26] J. Yao et al., "Tunable water-based meta-lens," *Advanced Optical Materials*, vol. 12, no. 6, p. 2300130, 2024.
- [27] R. Zhu and J. Wang, "A shape-changeable antenna constructed by distilled water for low profile and low radar cross-section applications," *IEEE Antennas and Wireless Propagation Letters*, 2023.
- [28] L. Xing, Y. Huang, S. S. Alja'afreh, and S. J. Boyes, "A monopole water antenna," in *2012 Loughborough Antennas Propagation Conference (LAPC)*, Nov. 2012, pp. 1–4.
- [29] C. Hua and Z. Shen, "Shunt-excited sea-water monopole antenna of high efficiency," *IEEE Transactions on Antennas and Propagation*, vol. 63, no. 11, pp. 5185–5190, Nov. 2015.
- [30] E. Paraschakis, H. Fayad, and P. Record, "Ionic liquid antenna," in *IWAT 2005. IEEE International Workshop on Antenna Technology: Small Antennas and Novel Metamaterials*, Mar. 2005, pp. 552–554.
- [31] H. Fayad and P. Record, "Broadband liquid antenna," *Electronics Letters*, vol. 42, no. 3, pp. 133–134, Feb. 2006.
- [32] C. Hua, Z. Shen, and J. Lu, "High-efficiency sea-water monopole antenna for maritime wireless communications," *IEEE Transactions on Antennas and Propagation*, vol. 62, no. 12, pp. 5968–5973, Dec. 2014.
- [33] S. G. O'Keefe and S. P. Kingsley, "Tunability of liquid dielectric resonator antennas," *IEEE Antennas and Wireless Propagation Letters*, vol. 6, pp. 533–536, 2007.
- [34] R. Zhou, H. Zhang, and H. Xin, "A compact water-based dielectric resonator antenna," in *2009 IEEE Antennas and Propagation Society International Symposium*, Jun. 2009, pp. 1–4.
- [35] R. Zhou, H. Zhang, and H. Xin, "Liquid-based dielectric resonator antenna and its application for measuring liquid real permittivities," *IET Microwaves, Antennas & Propagation*, vol. 8, no. 4, pp. 255–262, Mar. 2014.
- [36] M. Wang and Q. Chu, "High-efficiency and wideband coaxial dual-tube hybrid monopole water antenna," *IEEE Antennas and Wireless Propagation Letters*, vol. 17, no. 5, pp. 799–802, May 2018.
- [37] J. Liang, G. Huang, K. Qian, S. Zhang, and T. Yuan, "An azimuth-pattern reconfigurable antenna based on water grating reflector," *IEEE Access*, vol. 6, pp. 34 804–34 811, 2018.
- [38] Z. Hu, S. Wang, Z. Shen, and W. Wu, "Broadband polarization-reconfigurable water spiral antenna of low profile," *IEEE Antennas and Wireless Propagation Letters*, vol. 16, pp. 1377–1380, 2017.
- [39] Z. Hu, Z. Shen, and W. Wu, "Reconfigurable leaky-wave antenna based on periodic water grating," *IEEE Antennas and Wireless Propagation Letters*, vol. 13, pp. 134–137, 2014.
- [40] S. Wang et al., "A frequency-reconfigurable inverted-L antenna made of pure water," *IEEE Antennas and Wireless Propagation Letters*, vol. 21, no. 1, pp. 109–113, 2021.
- [41] Y. Li and K. Luk, "A water dense dielectric patch antenna," *IEEE Access*, vol. 3, pp. 274–280, 2015.
- [42] J. Sun and K. Luk, "A wideband low-cost and optically transparent water patch antenna with omnidirectional conical beam radiation patterns," *IEEE Transactions on Antennas and Propagation*, vol. 65, no. 9, pp. 4478–4485, Sept. 2017.
- [43] A. R. L. Colas, *Silicones: Preparation, Properties and Performance*, 2005.
- [44] R. B. V. B. Simorangkir et al., "Polydimethylsiloxane-embedded conductive fabric: Characterization and application for realization of robust passive and active flexible wearable antennas," *IEEE Access*, vol. 6, pp. 48 102–48 112, 2018.
- [45] R. E. Collin, *Field Theory of Guided Waves*, vol. 5, John Wiley & Sons, 1990.
- [46] K. P. Thakur and W. S. Holmes, "Reflection of plane wave from multi-layered dielectrics," in *APMC 2001. 2001 Asia-Pacific Microwave Conference (Cat. No. 01TH8577)*, vol. 2, Dec. 2001, pp. 910–913.
- [47] K. Ito, K. Furuya, Y. Okano, and L. Hamada, "Development and characteristics of a biological tissue-equivalent phantom for microwaves," *Electronics and Communications in Japan (Part I: Communications) Banner*, vol. 84, no. 4, pp. 67–77, Apr. 2001.
- [48] A. S. M. Sayem et al., "An electronically-tunable, flexible, and transparent antenna with unidirectional radiation pattern," *IEEE Access*, vol. 9, pp. 147 042–147 053, 2021.